Formulation and resolution of inverse problems for nonlinear, transient structural dynamics

François M. Hemez — Scott W. Doebling

Engineering Analysis Group (ESA-EA)
Los Alamos National Laboratory, P.O. Box 1663, M/S P946
Los Alamos, New Mexico 87545, U.S.A.
hemez@lanl.gov, doebling@lanl.gov

ABSTRACT. *A general framework is proposed for validating numerical models for nonlinear, transient dynamics. Previous work has focused on nonlinear vibration and several difficulties of formulating and solving inverse problems for nonlinear dynamics have been identified. Among them, we cite the necessity to satisfy continuity of the response when several finite element optimizations are successively carried out and the need to propagate variability throughout the optimization of the model's parameters. Our approach is illustrated using data from a nonlinear vibration testbed and an impact test experiment both conducted at Los Alamos National Laboratory in support of the advanced strategic computing initiative and our code validation and verification program.*

RÉSUMÉ. *Une formulation générale est proposée afin de valider les modèles numériques développés pour les besoins de la dynamique transitoire et nonlinéaire. Le travail réalisé antérieurement s'est concentré sur les applications en vibrations nonlinéaires et plusieurs difficultés ont été identifiées quant à la formulation et la résolution de problèmes inverses. Parmi ces difficultés, nous citons la nécessité de satisfaire la continuité des réponses temporelles lorsque plusieurs optimisations successives sont réalisées ainsi que le besoin de propager des sources de variabilité durant l'optimisation des paramètres du modèle. Nos conclusions sont illustrées à l'aide de données expérimentales issues d'un système vibratoire nonlinéaire et d'un système soumis à impact, tous deux développés et testés dans le cadre d'un programme initié à Los Alamos National Laboratory pour les validation et vérification des modèles numériques et phénomènes physiques complexes.*

KEY WORDS: *Nonlinear, transient dynamics, inverse problem, model updating.*

MOTS-CLÉS: *Dynamique nonlinéaire et transitoire, problème inverse, recalage.*

Nomenclature

The «Standard Notation for Modal Testing & Analysis» is used throughout this paper, see Reference [LIE 92]. Symbols not commonly used in the modal testing and structural dynamics communities are defined in the text.

1. Introduction

Inverse problem solving is at the core of engineering practices as such work generally involves designing a system to target a given performance or to satisfy operating constraints. Increasingly, designers are faced with shorter design cycles while their testing capabilities are reduced and the physics they must understand becomes more sophisticated. The consequence is the need for larger-size computer models, coupled-field calculations and more accurate representations of the physics. To improve the predictive quality of numerical models and enhance the capability to extrapolate the response of a system, it is often necessary to solve inverse problems where simulations are compared to field measurements [HEM 99a]. In addition, it has been recognized that non-deterministic approaches must be employed to alleviate our lack of test data and incomplete understanding of complex mechanics [HEM 99b].

In this work, a general formulation of inverse problems for correlating transient dynamics to responses obtained from several nonlinear finite element models is proposed. An application to the field of structural dynamics is described where several software packages are interfaced to enable fast probability integration using nonlinear finite element analysis [CRU 89]. Hence, probabilistic response surfaces and sensitivity data are generated for optimizing the structural form and design parameters of a family of models with the ultimate goal of identifying the best possible representation of the system.

The current application features the impact of a steel cylinder that compresses a layer of elastomeric material otherwise difficult to characterize with conventional testing procedures [BEA 99]. By correlating the transient acceleration response to field measurements, this behavior is characterized and high-fidelity, physics-based modeling of the material is optimized. In the effort to reproduce the test data, several models are developed by varying, among other things, the constitutive law and the type of modeling. Therefore, the optimization variables consist of the usual design variables augmented with structural form parameters such as kinematic assumptions and geometry description (2D or 3D). First, probabilistic sensitivity analysis is employed to identify the most important optimization parameters. Then, several metrics for comparing test and analysis data are evaluated. Finally, optimization is carried out to validate each one of the candidate models.

2. Motivations and Main Findings

We wish to convince the reader that, for a wide variety of test-analysis applications, techniques based on linear dynamics and modal superposition are likely to fail. Thus, it is critical to validate numerical models by correlating transient test data rather than steady-state, modal data. However, formulating correctly the inverse problem in this case requires to solve multiple two-point boundary value problems, as explained in Reference [DIP 98]. Our preliminary investigation of these techniques indicates that their computational requirements prohibit their application to the types of problems we are interested in. Instead, inverse problem solving is replaced by a methodology where response surfaces are generated from the resolution of a large number of forward analyses. This best utilizes our capabilities for modeling nonlinear systems using general purpose finite element packages [ABA 98] and our computational resources where parallel processing enables the simultaneous analysis of several thousand nonlinear problems very efficiently. Two other important contributions to this work are 1) the ability to derive high accuracy, physics-based material models and 2) fast probability integration for large-scale structural analysis [NES 96]. The former is not discussed in this paper but it is briefly mentioned here because physics-based models of material behavior are generally obtained from a microscopic description of the material. As such, they depend on parameters that can not be measured with great accuracy and that are best characterized by probabilistic distributions. This explains why fast probability integration techniques are critical to our work and why optimization algorithms are required, not only to adjust parameters of the models, but also to assess the quality of models in a probabilistic sense. This procedure is summarized in Figure 1 where arrows symbolize the flow of information during the successive steps of testing, modeling, analysis and validation.
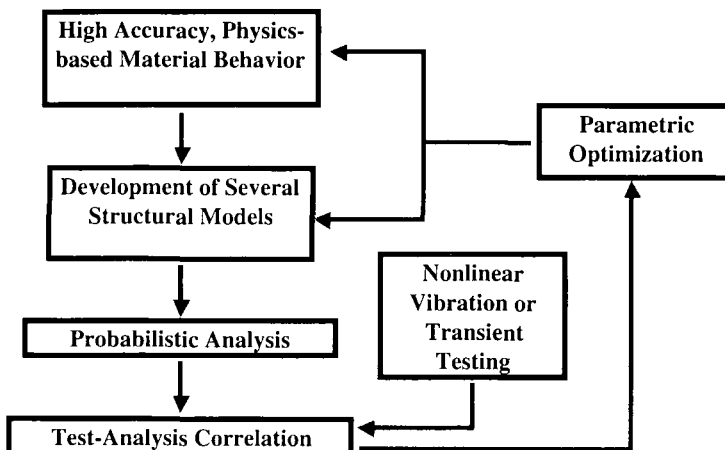
Figure 1. *The different steps of testing, modeling, analysis and validation*

In this way, the research effort presented here is mostly concerned with interfacing several general-purpose software packages together and learning how to utilize tools that have not necessarily been developed for test-analysis correlation and model validation. In doing so, however, we believe that this work contributes to open research issues such as assessing the efficiency of current metrics for test-analysis correlation, formulating inverse problems for nonlinear dynamics and developing a new testing procedure for characterizing nonlinear materials in the high deformation and high rate ranges. An important finding that we would like to emphasize and that will be addressed in future research is the need to develop new test-analysis correlation metrics (which is sometimes referred to as «feature extraction») for analyzing nonlinear, transient data. Another critical issue is the notion of model validation that can be, we believe, recast as a general pattern recognition problem [BIS 98].

2.1 Background

The first part of this research effort is documented in References [HEM 99a], [HEM 99b] and has consisted in attempting to formulate criteria for measuring the correlation between test data and finite element results for nonlinear vibrations. Since we have always constrained ourselves to 1) handle any type and source of nonlinearity and 2) enable both parametric and non-parametric updating to be carried out simultaneously, very few techniques have been found in the published literature that could meet our expectations. Typical examples of nonlinearities we are interested in include material nonlinearity, friction, impact and contact at the interface between two components. These are typical of nonlinearity sources dealt with in the automotive and aerospace industries. As an illustration of this lack of techniques relevant to the nonlinear word, the reader is invited to review from References [IMR 91], [MOT 93] the state-of-the-art in model updating technology. Among the earliest and most promising work in test-analysis correlation for nonlinear dynamics, we cite the work by Hasselman and Anderson [HAS 98] and that by Dippery and Smith [DIP 98].

2.2. Experimental Testbed for Nonlinear Vibrations

Our testbed for the validation of nonlinear vibration modeling is the LANL 8-DOF (which stands for Los Alamos National Laboratory eight degrees of freedom) system illustrated in Figure 2. It consists of eight masses connected by linear springs. The masses are free to slide along a center rod that provides support for the whole system. Modal tests were performed on the nominal system and on a damaged version where the stiffness of various springs is reduced by 14 %. A contact mechanism was also added between two masses to induce a source of contact/impact, see Figure 2. Time-domain acceleration data are measured at each

one of the eight masses and modal parameters are identified using a classical frequency-domain curve fitting algorithm.
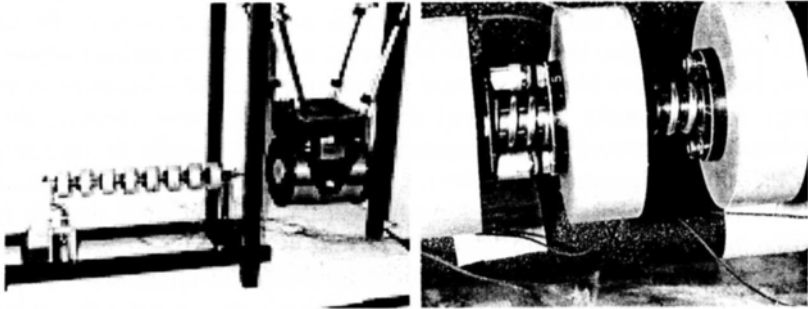
Figure 2. *LANL 8-DOF Testbed. Overall setup (left) and detail (right)*

2.3. *Application of Modal-based Updating Techniques*

The test we are interested in consists of identifying the damaged spring using a linear model that does not account for the friction nor the source of contact/impact. This is achieved by minimizing the «distance» between test data and predictions of the numerical model, whether this distance is evaluated in the time or frequency domain. The optimization problem can be formulated as the minimization of the cost function shown in equation [1] where the first contribution represents the metrics used for test-analysis correlation and the second contribution serves the purpose of regularization

$$\min_{\{dp\}} \sum_{j=1\cdots N_{test}} \left\{R_j(p+dp)\right\}^* \left[S_{RR_j}\right]^{-1} \left\{R_j(p+dp)\right\} + \{dp\}^T \left[S_{pp}\right]^{-1} \{dp\} \quad [1]$$

Constraints are added to the formulation to eliminate any local minimum that would not be acceptable from a physical standpoint. In this test, the parameters of interest are the seven spring stiffnesses. The weighting matrices in equation [1] are generally kept constant and diagonal for computational efficiency. They can also be defined as general covariance matrices which formulates a Bayesian correction procedure, as shown in Reference [HEM 99b]. Obviously, many choices for the metric are available, the simplest of all being the difference between test and analysis modal parameters, also known in the model updating community as the output error residual, see Reference [PIR 91].

The results summarized here involve the definition of the output residue [PIR 91] and two input residues, namely, the force and hybrid modal residues defined in References [HEM 95] and [CHO 98]. We emphasize that our purpose is not to compare various figures of merit for their efficiency to identify sources of modeling

error but rather to illustrate the danger of modal-based updating when the system is characterized by a source of nonlinearity not accounted for by the numerical model. Here, for example, friction is not represented. Although the linear model provides a good agreement with test data before and after parametric correction, the update fails to yield a positive identification of damage introduced at spring number five. Worse, false positives (that is, stiffness reductions predicted at locations where no damage was originally introduced) are obtained. We have checked that the optimization solvers used are not responsible for these poor results. In this study, the order-0, Simplex algorithm, the order-1, conjugate gradient algorithm and the order-2, BFGS and Levenberg-Marquardt methods are implemented and they all fail to identify the damage scenario when associated to modal-based metrics. These classical optimization solvers are described in many publications and manuscripts among which we cite Reference [JAC 77]. This simply demonstrates the limitations of modal data to characterize nonlinear dynamics.

2.4. *Time-domain Correlation Metrics*

The next step is to implement two correlation metrics based on time series and described in Reference [HEM 99a]. The first one correlates the measured and simulated signals directly (RMS error) while the second one correlates the subspaces to which these signals belong. This is achieved by making the numerical model match the singular values and vectors obtained by decomposition of the test data matrix, a procedure generally referred to as principal component decomposition (PCD). Reference [HAS 98] offers a complete description of this procedure. The main result is that time-domain metrics are successful at identifying parametric and/or non-parametric errors even when the model optimized is purely linear.

For example, we can identify the nonlinear, internal force by minimizing the RMS or PCD error based on acceleration measurements at three locations only. Here, the contact mechanism is enabled, therefore, introducing a source of contact/impact during the vibrations. The random, input excitations at the driving point (location 1) and the eight accelerations are measured at 4,096 samples over a time period of 8 seconds. Data are collected for various force levels to identify the degree of nonlinearity. Although all degrees of freedom are measured, we assume that data are available at locations 1, 5 and 6 only. Since the correlation involves three measurements only, model reduction is implemented to condense the finite element matrices and force vectors. The particular technique chosen preserves exactly the lowest frequencies and mode shapes of the linear model [BUR 94]. As mentioned previously, our modeling of this system is perfectly linear except for the addition of an internal force vector. Arbitrary internal forces are applied at each one of the eight masses of the system and test-analysis correlation is used for estimating these force levels at prescribed time samples. The unknowns are therefore these eight force components. Correlation is based on the first 90 acceleration

measurements that span the time window [0;0.168] sec. For the numerical simulation, finite element matrices and force vectors are reduced to the size of the test model (locations 1, 5 and 6 only) and the response of the condensed model is integrated in time using 10 sampling points between any two measurements. As the response is integrated in time, the internal force vector is optimized. Figure 3 shows the reconstruction of internal force as optimizations are performed for each time interval containing three consecutive measurements. In other words, 30 optimizations are performed, one every 0.0056 sec. No clear interpretation of this forcing function can be made. Notice that the internal force at location 1 is approximately equal to zero which seems consistent with the fact that degree of freedom 1 is the driving point where the random excitation is applied.
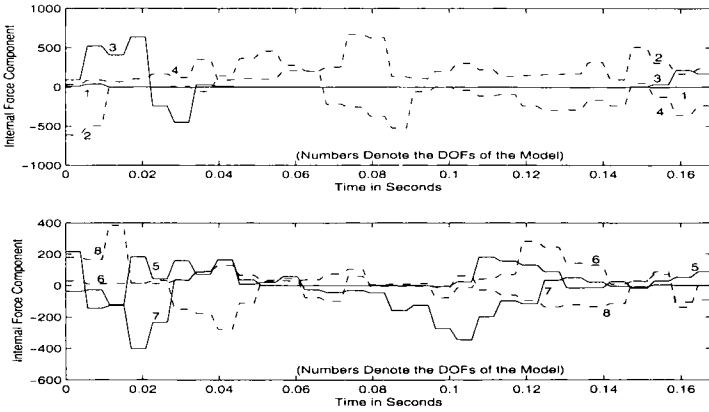
Figure 3. *Internal force reconstructed via test-analysis correlation*

Figure 4 illustrates the correlation before and after model updating when the cost function is defined by the RMS error. Similar results are obtained using the PCD metric. Adding to the numerical simulation the nonlinear force identified via test-analysis correlation (see Figure 3) provides a clear improvement of the model's predictive quality. This simple example illustrates how unmodeled dynamics can be identified in the context of incomplete measurement sets and nonlinear responses. The next step is to show in Section 3 below that large numerical models can be validated using similar test-analysis correlation metrics, explicit, time-domain solvers and probability integration.
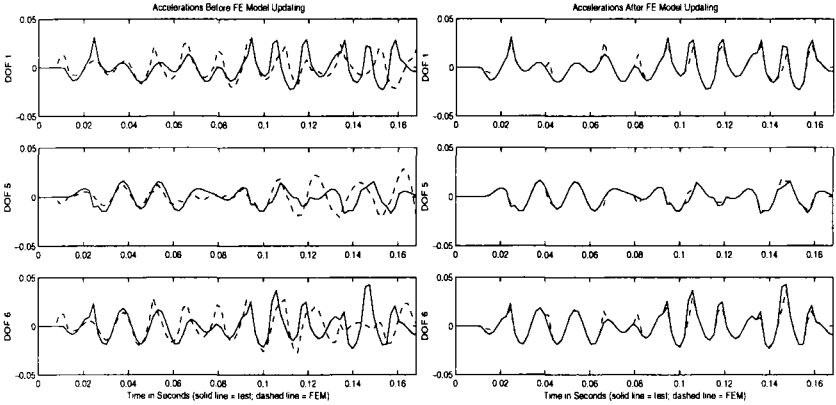
Figure 4. *Accelerations before (left) and after (right) optimization*

2.5. *Discontinuity of the Solution Fields*

When time-domain data are used for validating a numerical model, it may be advantageous to divide the available time record into several windows, each of smaller duration. The reason is that the computational effort of calculating a cost function in the time domain is directly proportional to the number of increments required to integrate the equation of motion. The shorter the time window, the faster the optimization. However, the strategy of implementing successive optimizations produces several optimized models, one for each time window considered. This is necessary not only for computational purposes but also because some of the parameters being optimized may vary in time and following such evolution as it occurs may be critical. However, nothing in the formulation of the inverse problem enforces continuity between the solution fields obtained from models optimized in two successive time windows. Since the optimization variables can converge to two different solutions, the discontinuity of the solution can be written, for example, as

$$\lim_{\substack{t \to t_i \\ t \le t_i}} x(p^{(i)}, t) \ne \lim_{\substack{t \to t_i \\ t \ge t_i}} x(p^{(i+1)}, t) \qquad [2]$$

Optimal control strategies can be implemented to solve the inverse test-analysis correlation problem while reconstructing continuous solution fields and identifying the source of modeling error, as explained in References [DIP 98] and [MOO 89]. They rely on the resolution of multiple two-point boundary value problems (BVP). When satisfactory solutions to the two-point BVP's are obtained, it is guaranteed that the numerical model matches the measured data at the beginning and at the end of the time window considered for the optimization. The optimal error control is a very attractive technique since not only does it handle parametric and non-parametric identifications simultaneously but it also propagates uncertainty and

variability using the Bayesian theory of information and it provides a rigorous framework for generating continuous solutions from an arbitrary number of optimizations.

However, this improvement comes with the additional cost of formulating a two-point BVP to guaranty continuity of the solution. Since the procedure is embedded within an optimization solver, multiple two-point BVP's must be solved for. Unfortunately, the impact on the computational requirement is enormous. For example, our resolution of the single degree of freedom, Duffing oscillator problem shown in Reference [DIP 98] requires a total of 16 to 20 hours of CPU time depending on the number of measurement points available. This timing is obtained on a dedicated R10,000/250 MHz processor when the algorithm is programmed within the environment provided by Matlab™ [MAT 99]. Clearly, it prohibits any application of the technique to practical engineering problems. This is why other avenues are explored in the remainder of this paper.

3. Impact Test Experiment

The application targeted is a high-frequency shock test that features a component characterized by a nonlinear, visco-elastic material behavior. Our intent is to validate an existing elastomeric material model. Since the original testing procedure that provided this model was quasi-static, it is our belief that the model does not represent the behavior with good fidelity at high strain rates.

3.1. *Numerical Modeling*

An illustration of the setup is provided in Figure 5. In an effort to match the test data, several FE models are developed by varying, among other things, the constitutive law and the type of modeling. Therefore, optimization variables consist of the usual design variables augmented with structural form parameters such as kinematic assumptions, geometry description (2D or 3D), contact modeling and numerical viscosity. Figure 5 also illustrates one of the discretized models used for numerical simulation. The analysis program used for the calculations is HKS/Abaqus-Explicit, a general-purpose package for finite element modeling of nonlinear structural dynamics [ABA 98]. It features an explicit time integration algorithm convenient when dealing with nonlinear material behavior, potential sources of contact and high frequency excitations.
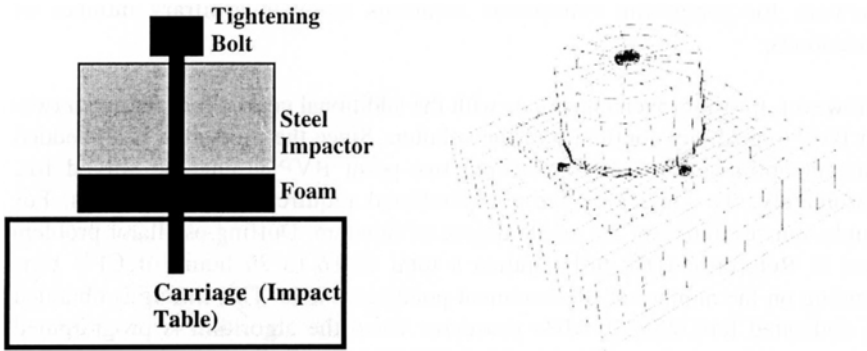
Figure 5. *Assembly of the impactor and carriage (left) and 3D model (right)*

It can be observed from Figure 5 that the main two components (steel impactor and foam layer) are assembled and attached to the carriage. The center of the steel cylinder is hollow and is fixed with a rigid collar to restrict the motion of the impactor to the vertical direction. This assures perfectly bilinear contact between the steel and foam components, allowing the structure to be modeled axi-symmetrically. In spite of this, a full three-dimensional model is also developed to verify this assumption. Another important parameter is the preload applied by the bolt used to hold this assembly together. The torque applied was not measured during testing and it may have varied from test to test.

3.2. Experiment Setup

During the actual test, the carriage that weighs 955 lbm (433 kg) is dropped from various heights and impacts a rigid floor. The input acceleration is measured on the top surface of the carriage and three output accelerations are measured on top of the steel impactor that weights 24 lbm (11 kg). Figure 6 provides an illustration of the test setup and instrumentation. This impact test is repeated several times to collect multiple data sets from which the repeatability of the experiment can be assessed. Upon impact, the steel cylinder compresses the foam to cause elastic and plastic strains during a few μ-seconds.
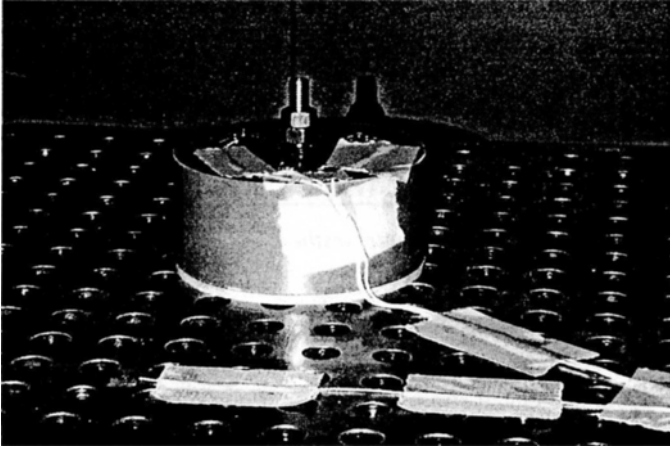
Figure 6. *LANL impact test setup*
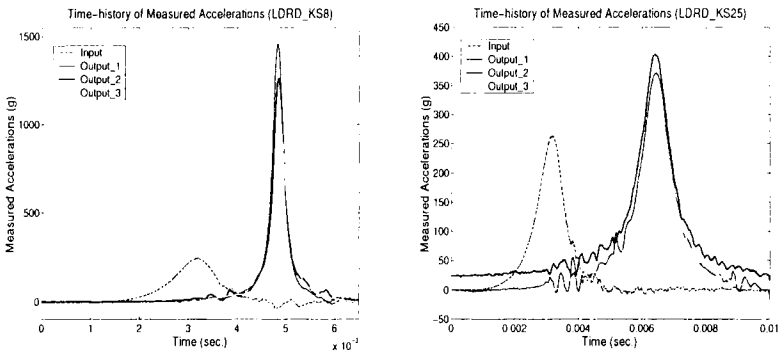
Figure 7. *Accelerations measured during the impact test. Low-velocity impact of a thin layer of material (left) and a thick layer of material (right).*

Typical accelerations measured during the impacts are depicted in Figure 7. Both data sets are generated by dropping the carriage from an initial height of 13 inches (0.33 meters). On the left of Figure 7, the acceleration response of a 1/4 inch-thick (6.3 mm) layer of foam is shown. On the right, the acceleration response of a 1/2 inch-thick layer (12.6 mm) is shown. The results available are summarized in Table 1 which gives the number of data sets collected for each configuration tested. The reason why less data sets are available at high impact velocity is because these tests proved to be destructive to the elastomeric material and could not, therefore, be repeated to study the variability.

Number of Data Sets Collected	Low Velocity Impact (13 in./0.3 m Drop)	High Velocity Impact (155 in./4.0 m Drop)
Thin Layer (0.25 in./6.3 mm)	10 Tests	5 Tests
Thick Layer (0.50 in/12.6 mm)	10 Tests	5 Tests

Table 1. *Data collected with the impact testbed*

It can be seen that over a thousand g's are measured on top of the impact cylinder which yields large deformations in the foam layer. The time scale also indicates that the associated strain rates are important. Lastly, the variation in peak acceleration observed in Figure 7 suggests that a non-zero angle of impact is involved, making it necessary to model this system with a 3D discretization. Clearly, modal superposition techniques would fail modeling this system because: 1) contact can not be represented efficiently from linear mode shapes; 2) nonlinear hyper-foam models, that possibly include visco-elasticity, are needed to represent the foam's hardening behavior; 3) very refined meshes would be required to capture the frequency content well over 10,000 Hz.

4. Validation of Nonlinear Structural Dynamics Models

In this Section, the overall procedure for test-analysis correlation (TAC) is described with emphasis on explaining how the problem of probabilistic model validation is formulated. For this reason, technical details are eluded as much as possible. These can be found in the References cited throughout this work.

4.1. *Response Surfaces for TAC & Optimization*

As mentioned previously, correctly formulating inverse problems based on time-domain data requires the resolution of multiple two-point boundary value problems within the parameter adjustment loop [DIP 98]. This formulation yields prohibitive computational costs for the systems we are interested in. The alternative pursued here is to, first, generate a response surface from a large number of explicit FE solutions. A typical sampling technique used is the Latin hypercube method. If additional resolution is required, curve-fitting or neural networks can be implemented for interpolating between data points. Once the FE solutions are available for multiple designs, a metric is adopted to correlate the time-domain data. In this work, essentially three metrics are defined: 1) comparing peak acceleration values; 2) comparing time-histories of acceleration data; 3) the PCD method mentioned in Section 2. The cost functions (also referred to as « g-function » in the

next Section) associated with these three metrics are described by equations [3], [4] and [5], respectively:

$$g(X) = \left(\max\left(\ddot{x}_s\right) - \max\left(\ddot{x}_s^{\text{test}}\right)\right)^2 \qquad [3]$$

$$g(X) = \sum_{s,\text{sensor}} \sum_{t,\text{time}} \left(\ddot{x}_s(t) - \ddot{x}_s^{\text{test}}(t)\right)^2 \qquad [4]$$

$$g(X) = \frac{1}{N_o^2} \sum_{i=1\cdots N_o} \sum_{j=1\cdots N_o} d\Phi_{ij}^2 + \frac{1}{N_o} \sum_{i=1\cdots N_o} d\sigma_i^2 + \frac{1}{N_o N_t} \sum_{i=1\cdots N_o} \sum_{j=1\cdots N_t} d\Psi_{ij}^2 \qquad [5]$$

where $\{X\}$ denotes the subset of design parameters and/or random variables selected for parametric adjustment. Symbols used in equation [5] represent normalized differences between the singular values and singular vectors of the analysis and test data matrices. The definition of other metrics or «features» for nonlinear dynamics is an aspect on which we are increasingly focusing.

4.2. *Fast Probability Integration*

Our ability to perform probabilistic structural analysis relies essentially on the software NESSUS (which stands for Numerical Evaluation of Stochastic Structures Under Stress), see Reference [NES 96], and its fast probability integration (FPI) capability is described here.

In the following, it is assumed that N random variables collected in vector $\{X\}$ must be defined in the model. These may include uncertain input forces, random parameters for material modeling, manufacturing tolerances, etc. We also define a response function Z and the objective of the FE calculation is to estimate the value of Z for a given sample $\{X\}$ of our random variables. Finally, a limit state function $g(X)$ is defined that describes the correlation with test data. For reliability analysis, the g-function represents a limit on the acceptable behavior of the system. It is used for separating the safe domain (when $g(X) \geq 0$) from failure (when $g(X) < 0$). Here however, the g-function represents the metric used for test-analysis correlation. A simple illustration is provided in the following where the response Z is defined as the peak acceleration at a location coincident with a sensor and the g-function includes the peak acceleration value measured at that location during the test. In this particular case, the figure-of-merit defined for validating candidate models is simply given by equation [3]. «Success» is defined if $g(X) = 0$, that is, if the peak acceleration measured during the test is matched by the model in a probabilistic sense. This essentially means that the problem of model validation consists of calculating either the probability density function (PDF) or the cumulative density function (CDF) of the Z-response, respectively defined as

$$p_Z(a) = \text{Prob}[Z = a], \quad F_Z(\alpha) = \text{Prob}[Z \leq \alpha] = \int_{-\infty}^{\alpha} p_Z(z)dz \qquad [6]$$

Hence, FPI is used to propagate efficiently variability information through a structural analysis. Typically, estimating the entire PDF with a FE model that depends on N random variables requires no more than (N+1) analyses using FPI. The central aspect of FPI is the search for the most probable point (MPP) that defines the most probable prediction of the model in the presence of modeling uncertainty. To find the MPP, the algorithm maximizes the joint PDF in variables $\{X\}$ subject to the constraint $g(X)=0$. A critical computational issue is the transformation of random variables $\{X\}$ into standardized normal variables $\{u\}$, that is, variables described by the unit normal CDF

$$\Phi(u) = \int_{-\infty}^{u} \frac{1}{\sqrt{2\pi}} e^{-\frac{s^2}{2}} ds \qquad [7]$$

This is achieved via the Rosenblatt Theorem (see Reference [ROS 52]) that states that multivariate random variables can be converted to uniform distributions, then, to unit Gaussian distributions

$$u = \Phi^{-1}(F_Z(X)), \quad X = F_Z^{-1}(\Phi(u)) \qquad [8]$$

This additional step facilitates greatly the search for the MPP and all subsequent calculations. A final aspect of the computational procedure is that, during the optimization, the constraint $g(u)=0$ may be approximated using various polynomials to decrease the computational burden. Once the MPP has been determined, the response surface can be explored to reconstruct the entire PDF.

4.3. *Software Integration*

Software integration is an important part of our probabilistic model validation procedure. First, the optimization parameters and random variables are defined. Multiple FE solutions and multi-dimensional response surfaces are generated from statistical sampling. The first useful result is the sensitivity analysis used to reduce the subset of potential optimization variables down to the most sensitive ones. Then, the best model is sought after by optimizing the design parameters. The ability of a probabilistic model to reproduce test data is assessed using the Z-response's CDF. Of course, when multiple data sets are available, CDF's of the family of models must be compared to the CDF established from test data and not to individual measurements anymore. Three software packages involving four different programming languages are interfaced. The test-analysis correlation procedure is controlled by a library of Matlab™ functions [MAT 99]. The reason for this choice is flexibility and the possibility to develop a user graphical interface easily. Depending on the type of analysis requested by the user, the Matlab™-based software writes and compiles Fortran77 routines that are used for generating the Abaqus input deck. Drivers written in the script language Python [LUT 96] are also generated and used for piloting the FE analyses. Finally, results are uploaded back into Matlab™ for test-analysis correlation and parametric optimization. This

architecture should enable the interfacing in a near future of a variety of engineering analysis software, including parallel FE processing packages such as Lawrence Livermore National Laboratory's ParaDyn for running large-dimensional, nonlinear problems on high-performance computing platforms.

5. Demonstration of Model Validation With the Impact Testbed

An illustration of several concepts discussed previously is now provided with the data sets collected during the impact test experiment presented in Section 3. After describing the test data variability (Section 5.1), the model's predictive quality is assessed using fast probability integration (Section 5.2). The problem of measuring the consistency of two populations of data points is briefly addressed (Section 5.3). Model validation is performed in Section 5.4 by reconstructing response surfaces using two test-analysis correlation metrics and optimizing the design variables to get the best test-analysis match. Finally, the concept of model verification for nonlinear dynamics is illustrated (Section 5.5).

5.1. *Variability of the Experiment*

Figure 8 shows the variability observed during the impact test when the same configuration (same sample of elastomeric material and impact velocity) is tested ten times. Although the environment of this experiment was very well controlled, a small spread in both input and output signals is obtained. This justifies our point that model correlation and model validation must be formulated as statistical pattern recognition problems.
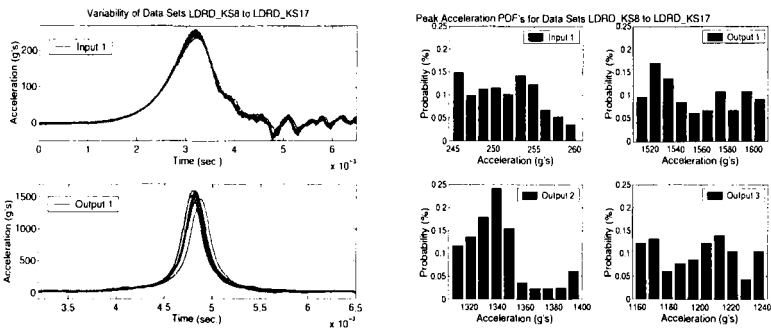

Figure 8. *Test data from 10 «similar» tests (left) and resulting PDF's (right)*

From these multiple measurement sets, variability of the test data can be assessed and represented in a number of ways, an illustration of which is provided on the

right of Figure 8. It shows the peak acceleration PDF's for each measurement. Such representation tells us, for example, that 17% of the peak accelerations measured at output sensor 1 are equal to 1,520 g's when «similar» experiments are repeated. According to Figure 8, this is the most probable peak acceleration. What is therefore important is not necessarily that the correlated models reproduce the peak acceleration measured during a single test, but that they predict the different acceleration levels with the same probability of occurrence as the one inferred from test data.

5.2. Analysis of the Probabilistic Models

The next step is to obtain the statistical characterization of numerical models. This is achieved via fast probability integration, as seen previously. The models are then individually validated by comparing their PDF's or CDF's to those obtained from test data. For this application, several 2D and 3D models are developed. Among the parameters varied are the type of elements used in the discretization, the mesh size, the type of contact conditions implemented, the material modeling, the preload applied when the center bolt is tightened, the velocity at time of impact and the input acceleration. The two types of information obtained by FPI are illustrated in Figure 9.
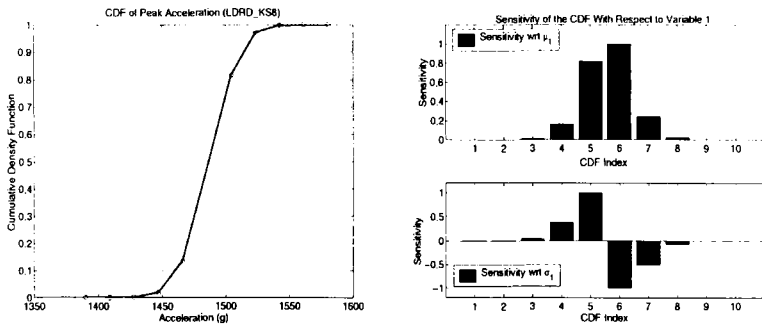

Figure 9. *CDF of the peak acceleration (left) and its sensitivity (right)*

After defining each one of the random variables, a relatively small number of FE solutions are needed to estimate, in this case, the probability distribution of the peak acceleration at output sensor 1. From Figure 9 (left), it can be seen, for example, that the probability that the peak acceleration is less than 1,520 g's is equal to 90%. These PDF or CDF vectors can also be differentiated with respect to each one of the random variables. It provides valuable information regarding the influence of a probability distribution on a cost function or Z-function for test-analysis correlation. Figure 9 illustrates this concept: the CDF shown on the left is differentiated with

respect to the mean of the velocity at time of impact (right, top half) and the standard deviation (right, bottom half) when it is assumed that the velocity is normally distributed. Peak acceleration values (on the horizontal axis) most sensitive to the impact velocity can then be identified.

The sensitivity information can be further condensed into single indicators that compare the influence of each random variable on the Z-function. Figure 10 summarizes a study where the influence of five variables (impact velocity, foam thickness, foam density and parameters of the stress-strain, hyperfoam model) is investigated. This information is used for selecting the most sensitive parameters in a manner similar to an analysis performed with a deterministic model. However, due to the nature of random variables, we emphasize that derivatives can not be estimated with respect to the variables themselves. Instead, their statistics must be used as illustrated in Figure 9.
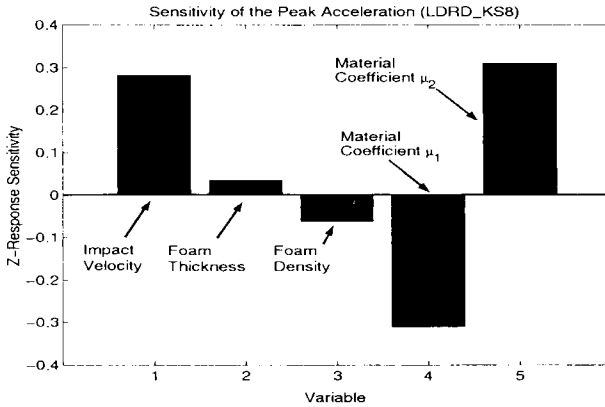
**Figure 10.** *Sensitivity of the CDF with respect to several random parameters*

Parameter Varied	Sensitivity Observed	Optimum Value/Range
Type of Elements	Very Low	CAX4R, C3D8R
Mesh Size	Very Low	1/10th Dimensions
Contact Condition	Very Low	Free, No Weights
Impact Velocity	Low	550 in./sec.
Steel Material	Low	304-SS
Angles of Impact	High	0.5 degrees
Bolt Preload	High	120-160 psi
Bulk Viscosity	High	0.5-0.8
Foam Material	Very High	1.2 x Stiffer
Input Scaling	Very High	1.2-1.6

Table 2. *Qualitative results of the probabilistic sensitivity studies*

Table 2 shows some of the sensitivity and optimization results obtained when the cost function [3] is implemented. These results are discussed below.

5.3. *Statistical Consistency of Test Data and Simulations*

One of the somewhat open research issues identified by this work is the problem of establishing a correlation between multiple data sets. By this we mean "assessing the degree to which two populations are consistent with each other." Our literature review seems to indicate that tools for assessing the distance between multivariate data sets are not readily available. This difficulty is illustrated in Figure 11. It represents the peak acceleration values for channels 1 and 2 plotted against each other. The data of ten independent, "identical" tests are shown together with simulation results generated by two different models. For each model, a particular design is generated by varying the angles of impact and the bolt preload. Then, each design is analyzed ten times using the ten different input acceleration signals measured during the repeated experiments. The three ellipsoids shown in Figure 11 illustrate the 95% confidence intervals for the test data and two models.
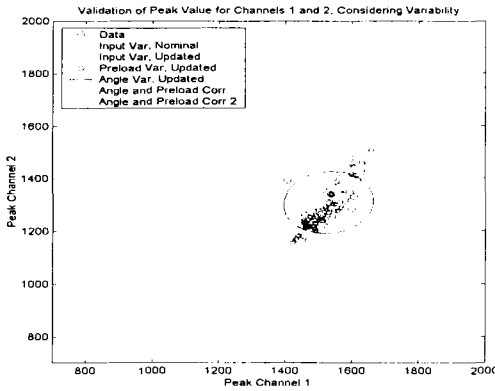
Figure 11. *Comparison of test and analysis data in a two-feature space (The 2D space represents the peak accelerations at sensors 1 and 2.)*

Obviously, the predictive quality of one of the two models is better because most of its data points (68 of 100) fall within the 95% confidence interval of the test data. The other model predicts only 34 of 100 points within the test's 95% confidence interval. This example illustrates that plotting several features against each other defines a more powerful analysis tool than a simple comparison of time-histories. Unfortunately, higher-order graphics are difficult to interpret visually. A quantitative indicator of the model's fit to test data is required when more than two features are

analyzed simultaneously. Two such statistical, «goodness-of-fit» indicators are briefly presented in the remainder.

By inspection of Figure 11, it is apparent that the peak magnitudes of accelerations 1 and 2 are uncorrelated because the 95% confidence interval is nearly circular. Thus, we suspect that one of the greater sources of variability is the source that affects the channels differently. This conclusion, however, is not confirmed by data generated from the two models. One of them clearly exhibits greater variability as indicated by the large confidence interval. The other one shows that the peak accelerations obtained are somewhat correlated even if the features are statistically consistent with test data. This can be assessed using a standard, multivariate Hotelling's T^2 test. First, statistics such as the vector of mean and the matrix of covariance can be evaluated from the distribution of features. Hotelling's T^2 test states that the model's mean vector is an estimate of the test data to the $(100-\alpha)\%$ confidence level if

$$\left(\{\mu(p)\} - \{\mu_{test}\}\right)^T \left[\Sigma_{test}\right]^{-1} \left(\{\mu(p)\} - \{\mu_{test}\}\right) \leq \frac{N_p\left(N_s - 1\right)}{N_s\left(N_p - 1\right)} F_{N_p, N_s - N_p}(\alpha) \quad [9]$$

Applied to the data shown in Figure 11, this statistic sets the acceptance ratio to 1.0035 at the 95% confidence level. The Mahalanobis distance in the left-hand side of equation [9] is equal to 4.0 for the first model which clearly indicates that it fails the test. The Mahalanobis distance of the second model is equal to 0.2. This establishes that the mean response predicted by our second model has converged. It can alternatively be stated that we are 95% confident that the average peak accelerations predicted by this model are consistent with test data given the sources of variability of the experiment and given the sources of modeling uncertainty. However, this conclusion remains of limited practical use as long as the variance of the population has not converged as well. One of the only possibility for testing both mean and variance is to calculate Kullback-Leibler's relative entropy defined as the expected value of the ratio between the PDF's of the two populations

$$I(Model \parallel Test) = E\left[\frac{p_Z^{model}(\alpha)}{p_Z^{test}(\alpha)}\right] \quad [10]$$

If the features used are normally distributed (or if enough data points are available to justify the application of the central limit Theorem), the relative entropy can be approximated as

$$I(\text{Model} \parallel \text{Test}) \cong \frac{1}{2} \left(\text{Trace}\left([\Sigma(p)][\Sigma_{\text{test}}]^{-1}\right) - N_p - \log\left(\frac{\det[\Sigma(p)]}{\det[\Sigma_{\text{test}}]}\right) \right) \quad [11]$$

$$+ \frac{1}{2} \left(\{\mu(p)\} - \{\mu_{\text{test}}\}\right)^T [\Sigma_{\text{test}}]^{-1} \left(\{\mu(p)\} - \{\mu_{\text{test}}\}\right)$$

This metric would typically be used for assessing the consistency between two populations of features and for optimizing parameters of the model. Unfortunately, statistical tests for verifying a pass/fail hypothesis based on the relative entropy [10-11] are not available in the general case. This limitation is currently being addressed. Another important issue is the availability of multiple data sets. For many applications, the experiment can not be repeated and the amount of measurements available is insufficient to establish meaningful statistics. The method of surrogate data offers an attractive solution, as demonstrated recently in Reference [PAE 99] with an application to nonlinear dynamics. It can be used for generating additional data sets after the original distributions have been converted to unit, Gaussian distributions via the Rosenblatt transform. By using the tools briefly discussed in this Section and by investigating multiple data features rather than simple comparisons of time-series, we believe that a systematic procedure for the qualification of modeling uncertainty can be developed based on test-analysis correlation whether a single test or repeated experiments are available.

5.4. *Parametric Optimization for Test-Analysis Correlation*

If the correlation with test data is not found satisfactory, Z-response surfaces are used to generate fast-running models. These, in turn, provide the core of the parametric optimization algorithm that fine-tunes a subset of the model's design variables to improve the correlation with test data. In this Section, a case is discussed where the nonlinear foam model, the bolt preload and the angles of impact are optimized.

Time measurements from the three sensors are gathered in a data matrix and its principal component decomposition is compared to numerical simulations. The three singular values obtained from test data are equal to 8.79e+06, 0.85e+06 and 0.13e+06 which clearly indicates that the dynamics is dominated by a single «mode.» Figure 12 represents the three left singular vectors (or pseudo-mode shapes) and right vectors (or time series) obtained from test data.
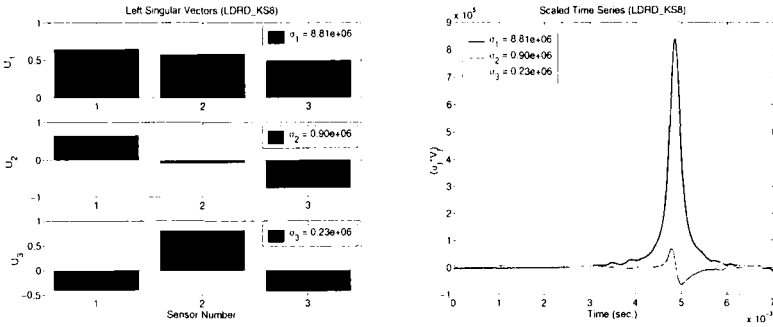
Figure 12. *Sets of left and right singular vectors from the PCD of test data. The pseudo-mode shape vectors shown on the left are normalized to unity. The time-series shown on the right are scaled by the corresponding singular values*

Although Figure 12 shows that the measured acceleration responses are dominated by a single «mode,» the contribution from the second PCD vector is far from insignificant. It means that the dynamics of the impact is somewhat more complicated than first thought, probably due to the motion of the foam pad relative to the impactor. From the left singular vectors, it can be deducted that the first mode corresponds to the rigid-body steel impactor compressing the foam pad because the vector exhibits roughly the same amplitude at each of the three sensors. The second vector indicates that the impactor/foam assembly features a small inclination compared to the carriage. From this second pseudo-mode shape, the location of the axis of rotation can be estimated. We have found that the angle provided by this calculation matches the angle obtained by numerical optimization (in the [0.5;0.7] degree range). The last vector probably involves elastic deformations of the steel impactor (first bending mode).

Figure 13 depicts a typical Z-response surface obtained with the 3D model: the two horizontal axes represent the values spanned by two parameters (an angle of impact and a scaling coefficient for the hyperfoam model) and the vertical axis represents the cost function [5] on a log scale. For clarity, the surface is shown as only two of the seven optimization variables are varied. The complete set includes two coefficients of the hyperfoam material model, two angles of impact that simulate a small free-play in the alignment of the carriage and steel impactor, the bolt preload, the input acceleration scaling factor and a numerical bulk viscosity parameter. A total of 1,845 FE models are analyzed to generate a fast-running model after having determined the approximate location of the cost function's minimum from probabilistic analysis. Figure 13 also depicts the test-analysis correlation before and after parametric optimization. A clear improvement of the model's predictive quality is witnessed. This is an important result because features used for
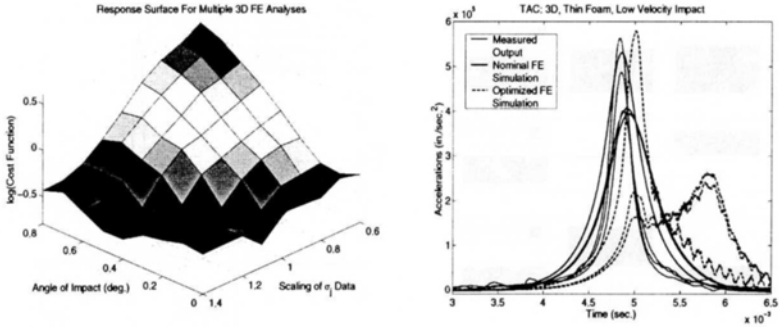
Figure 13. *Z-response surface (left) and correlation of the 3D model (right). (Test data are shown in red, solid line. Original predictions are shown in blue, dashed line. Predictions of the optimized model are shown in blue, solid line.)*

5.5. Verification of the Models

The last step consists in verifying that the optimized models are indeed correct. This is referred to as model verification here. It is achieved by comparing predictions of various models to measured data sets for configurations different from the one used during FPI and optimization. For example, the 3D models are optimized using the thin pad/low impact velocity setup. Then, the 2D, axi-symmetric models are verified with the thick pad/low impact velocity configuration. On the left-hand side of Figure 14, predictions of the original and final 2D models are compared to test data measured during a low-velocity impact using the 0.25 in. (6.3 mm) thick foam pad. On the right-hand side of Figure 14, the response of a 0.50 in. (12.6 mm) thick foam pad is featured. Despite small oscillations attributed to numerical noise generated by the contact algorithm, the models predict the acceleration levels measured during the test. We believe that such independent checks constitute the only valid proof that the modeling is correct.
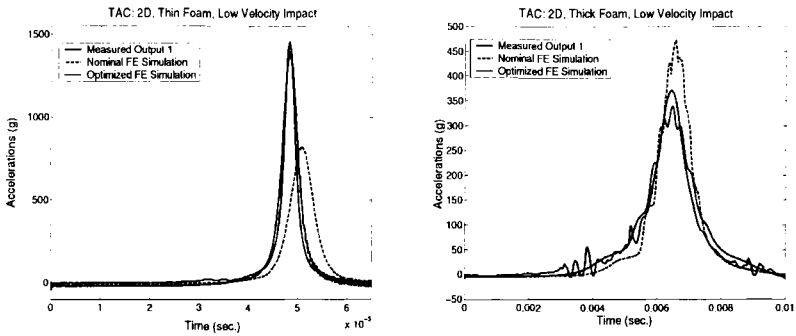
Figure 14. *Verification of the predictions. Left: response of a thin pad. Right: response of a thick pad. (Test data are shown in red, solid line. Predictions of the original model are shown in blue, dashed line. Predictions of the optimized model are shown in blue, solid line.)*

6. Conclusion

In this paper, a general framework is proposed for validating numerical models for nonlinear, transient dynamics. To bypass difficulties identified when applying test-analysis correlation methods to nonlinear vibration data, inverse problems are replaced with multiple forward, stochastic problems. After a metric has been defined for comparing test and analysis data, response surfaces are generated that can be used for 1) assessing in a probabilistic sense the quality of a particular simulation with respect to «reference» or test data and 2) optimizing the model's design parameters to improve its predictive quality. One critical issue to be investigated in future research is the definition of adequate metrics for correlating transient, nonlinear data. Rather than attempting to define deterministic, scalar distances, future work will emphasize dealing with «clusters» of test and analysis data that must be compared in a statistical sense.

7. References

[ABA 98] Abaqus/Explicit, User's Manual, Version 5.8, Hibbitt, Karlsson & Sorensen, Inc., Pawtucket, Rhode Island, 1998.

[BEA 99] BEARDSLEY P., HEMEZ F.M., and DOEBLING S.W., «Updating Nonlinear Finite Element Models in the Time Domain,» *Structural Monitoring 2000*, F.-K. Chang (Ed.), *2nd International Workshop on Structural Health Monitoring*, Stanford University, Stanford, California, Sep. 8-10, 1999, p. 774-783.

[BIS 98] BISHOP, C.M., *Neural Networks for Pattern Recognition*, Clarendon Press, Oxford University Press, Inc., New York, 1998.

[HAS 98]   Hasselman, T.K., Anderson, M.C., and Wenshui, G., «Principal Components Analysis For Nonlinear Model Correlation, Updating and Uncertainty Evaluation,» *16th SEM International Modal Analysis Conference*, Santa Barbara, California, Feb. 2-5, 1998, pp. 664-651.

[HEM 95]   Hemez, F.M., and Farhat, C., «Structural Damage Detection Via a Finite Element Model Updating Methodology,» *SEM International Journal of Analytical and Experimental Modal Analysis*, Vol. 10, No. 3, July 1995, pp. 152-166.

[HEM 99a] Hemez, F.M., and Doebling, S.W., «Test-Analysis Correlation and Finite Element Model Updating for Nonlinear, Transient Dynamics," *17th SEM International Modal Analysis Conference,* Kissimmee, Florida, Feb. 8-11, 1999, pp. 1501-1510.

[HEM 99b] Hemez, F.M., and Doebling, S.W., «A Validation of Bayesian Finite Element Model Updating for Linear Dynamics," *17th SEM International Modal Analysis Conference,* Kissimmee, Florida, Feb. 8-11, 1999, pp. 1545-1555.

[HEM 99c] Hemez, F.M., and Doebling, S.W., «Review and Assessment of Model Updating for Nonlinear, Transient Dynamics,» *Mechanical Systems and Signal Processing,* Special Issue EUROMECH-401, Inverse Methods in Structural Dynamics, Edited by J.E. Mottershead, November 1999, submitted.

[IMR 91]   Imregun, M., and Visser, W.J., «A Review of Model Updating Techniques,» *Shock and Vibration Digest*, Vol. 23, No. 1, 1991, pp. 19-20.

[JAC 77]   Jacobs, D.A.H., **The State of the Art in Numerical Analysis**, Ed., Academic Press, London, U.K., 1977.

[LIE 92]   Lieven, N.A.J., and Ewins, D.J., «A Proposal For Standard Notation and Terminology in Modal Analysis,» *10th SEM International Modal Analysis Conference,* San Diego, California, Feb. 2-5, 1992, pp. 1414-1419.

[LUT 96]   Lutz, M., **Programming Python**, O'Reilly & Associates, Inc., 1996.

[MAT 99] **Matlab™**, User's Manual, Version 5.3, The MathWorks, Inc., Natick, Massachusetts, 1999.

[MOO 89] Mook, D.J, «Estimation and Identification of Nonlinear Dynamic Systems,» *AIAA Journal*, Vol. 27, No. 7, July 1989, pp. 968-974.

[MOT 93] Mottershead, J.E., and Friswell, M.I., «Model Updating in Structural Dynamics: A Survey,» *Journal of Sound and Vibration*, Vol. 162, No. 2, 1993, pp. 347-375.

[NES 96]   **NESSUS**, User's Manual, Version 2.3, Southwest Research Institute, San Antonio, Texas, 1996.

[MOO 89] MOOK D.J, «Estimation and Identification of Nonlinear Dynamic Systems,» *AIAA Journal*, Vol. 27, No. 7, July 1989, p. 968-974.

[MOT 93] MOTTERSHEAD J.E., and FRISWELL M.I., «Model Updating in Structural Dynamics: A Survey,» *Journal of Sound and Vibration*, Vol. 162, No. 2, 1993, p. 347-375.

[NES 96] NESSUS, User's Manual, Version 2.3, Southwest Research Institute, San Antonio, Texas, 1996.

[PAE 99] PAEZ T., HUNTER N., and RED-HORSE J., «Statistical Tests of System Linearity Based on the Method of Surrogate Data,» *17th SEM International Modal Analysis Conference,* Kissimmee, Florida, Feb. 8-11, 1999, p. 1495-1500.

[PIR 91] PIRANDA J., LALLEMENT G., and COGAN S., «Parametric Correction of Finite Element Models By Minimization of an Output Residual: Improvement of the Sensitivity Method,» *9th SEM International Modal Analysis Conference*, Firenze, Italy, Jan. 1991.

[ROS 52] ROSENBLATT M., «Remarks on a Multivariate Transformation,» *The Annals of Mathematical Statistics*, Vol. 23, No. 3, 1952, p. 470-472.